On the role of AMOC weakening in shaping wintertime Euro-Atlantic atmospheric circulation

Climate Dynamics (2025) 63:273
https://doi.org/10.1007/s00382-025-07747-z

ORIGINAL ARTICLE

On the role of AMOC weakening in shaping wintertime Euro-Atlantic atmospheric circulation

Andrea Vito Vacca[1,2] · Katinka Bellomo[5] · Federico Fabiano[3] · Jost von Hardenberg[1,4]

Received: 10 January 2025 / Accepted: 22 May 2025 / Published online: 25 June 2025

Abstract
Climate change simulations project the slowdown of the Atlantic Meridional Overturning Circulation (AMOC) in the 21st century, though the rate and extent of the decline vary across models. In the Euro-Atlantic region, where the AMOC strongly influences sea surface temperature (SST) variability, climate projections also show significant uncertainty in the evolution of large-scale atmospheric circulation. We hypothesise that the decline of the AMOC and the uncertainty in Euro-Atlantic atmospheric circulation are interconnected. To test this, we analyse three coordinated experiments from the CMIP6 archive (SSP2–4.5, SSP5–8.5 and abrupt-4xCO2) adopting a storyline approach. In particular, we compare groups of models projecting a larger AMOC decline to groups of models projecting a smaller AMOC decline. Our results indicate that a stronger AMOC weakening is associated with an intensification of the North Atlantic storm track and jet stream, as well as an increased frequency of the NAO+ weather regime. We link these atmospheric changes to the influence of a reduced warming of the subpolar North Atlantic, known as the North Atlantic Warming Hole (NAWH), associated with the AMOC weakening. To further support our findings, we conduct an additional experiment using the EC-Earth3 model, comparing an abrupt-4xCO2 experiment with one where the AMOC is fixed at preindustrial levels. This experiment corroborates the CMIP6 analysis and validates our hypothesis. We conclude that the AMOC plays a critical role in driving atmospheric changes over the Euro-Atlantic region. Improved monitoring and better constraints on future AMOC decline would help reduce uncertainty in predictions of atmospheric circulation and climate impacts over Europe.

Keywords AMOC · Weather Regimes · North Atlantic · Jet stream

1 Introduction

The impact of anthropogenic forcing on mid-latitude atmospheric circulation is a growing societal concern. In the North Atlantic, large-scale atmospheric circulation shapes the trajectory and persistence of weather systems that affect densely populated areas of Europe, making it intrinsically linked to high-impact weather extremes (Woollings 2010; Pfahl 2014; Horton et al. 2015; Hoskins and Woollings 2015). Climate change simulations show the strengthening of the North Atlantic eddy-driven jet in winter (Oudar et al. 2020), leading to an eastern elongation of the North Atlantic storm track (Harvey et al. 2020), as well as a decrease in atmospheric blocking frequency (Davini and D'Andrea 2020). From a Weather Regimes perspective (Vautard 1990; Michelangeli et al. 1995), a warmer climate is also projected to result in an increased occurrence of the positive phase of the North Atlantic Oscillation (NAO+) (Fabiano et al. 2021). However, the inter-model spread in the circulation response is large, limiting our ability to make quantitative predictions of future changes and undermining confidence of climate change impacts over Europe (IPCC 2021; Shepherd 2014). A primary factor contributing to this uncertainty is the competing influence of different processes on the evolution of the equator-to-pole meridional temperature gradient,

✉ Andrea Vito Vacca
andrea.vacca@polito.it

1 Department of Environment, Land and Infrastructure Engineering, Polytechnic University of Turin, Turin, Italy

2 Istituto Universitario di Studi Superiori, Pavia, Italy

3 National Research Council, Institute of Atmospheric Sciences and Climate, Bologna, Italy

4 National Research Council, Institute of Atmospheric Sciences and Climate, Turin, Italy

5 Department of Geosciences, University of Padua, Padova, Italy

which controls the atmospheric baroclinicity and therefore the storm track and the jet (Shaw et al. 2016; Peings et al. 2017; Oudar et al. 2020; Harvey et al. 2014). The spotlight is on the tug-of-war between the accelerated warming of the Arctic (i.e. Arctic Amplification) and of the tropical upper troposphere (i.e. Upper Tropospheric Warming). The former reduces the low-level meridional temperature gradient, promoting a weaker, wavier mid-latitude jet stream (Coumou et al. 2018; Barnes and Screen 2015; Peings et al. 2017), while the latter increases the meridional temperature gradient in the upper levels promoting a strengthened and northward shifted jet (Rivière 2011; Harvey et al. 2014; Butler et al. 2010). The non-linear interaction between these two thermodynamic processes has been hypothesized to result in the projected squeezing of the wintertime North Atlantic jet, with an eastward elongation towards Europe (Peings et al. 2018). Other mechanisms, including cloud processes and the polar vortex, have also been invoked to explain future uncertainty in the North Atlantic circulation (Shaw et al. 2016). However, in this context, less attention has been given to the role of the ocean.

The Atlantic Meridional Overturning Circulation (AMOC) currently transports ~ 0.5 PW/year from the Southern Hemisphere into the North Atlantic, playing a vital role in shaping the present Earth's climate (Buckley and Marshall, 2016; Frierson et al., 2013; Henry et al., 2016; Lynch-Stieglitz, 2017; Rahmstorf, 2002; Clark et al., 2002). Throughout the 21st century, global climate projections consistently show a slowdown of the AMOC (Weijer et al. 2020) in response to changes in freshwater and heat fluxes in the North Atlantic and Arctic oceans (Nobre et al. 2023; Couldrey et al. 2023; Liu et al. 2019; Sévellec et al. 2017). However, the magnitude of the AMOC slowdown is highly model-dependent (Weijer et al. 2020; Fox-Kemper 2021). Bellomo et al. (2021) showed that the inter-model spread in the AMOC response to abrupt 4xCO2 forcing is a source of great uncertainty in the response of climate models to global climate change. In addition, the AMOC is considered a climate tipping element, with potentially devastating consequences for society and ecosystems if the system crosses a critical threshold (e.g. see recent review by Rahmstorf, 2024 and Armstrong McKay et al., 2022). Overall, the role of the AMOC in a context of climate change is still unclear, especially in the North Atlantic, where the AMOC has a strong influence on SST variability and related atmospheric impacts at various time-scales (Zhang et al. 2019; Oliveira et al. 2020; Bryden et al. 2014; Frankignoul et al. 2013; Borchert et al. 2018; Gastineau et al. 2013).

Previous work suggests that the AMOC is an important driver of Euro-Atlantic atmospheric circulation. For example, by analysing an ensemble of CMIP3 simulations, Woollings et al. (2012) concluded that the ocean—atmosphere coupling accounts for most of the projected intensification of the North Atlantic storm track. Building on, Chemke et al. (2022) identified the change in the dynamical coupling (i.e. ocean heat flux convergence) to be responsible for storm track intensification, pointing to changes in the ocean circulation. The climatic implications of an AMOC slowdown have been typically investigated using idealised experiments where the AMOC is weakened by imposing freshwater anomalies (water-hosing experiments). Independent simulations of this kind agree on the intensification and eastward elongation of the North Atlantic jet and storm track in response to a weakened AMOC (Bellomo et al. 2023; Liu et al. 2020; Jackson et al. 2015; Brayshaw et al. 2009). These impacts are consistent with the atmospheric response of an imposed North Atlantic Warming Hole (Gervais et al. 2019), a well-known surface temperature pattern in the Sub-Polar North Atlantic (SPNA), which is thought to be related to the weakening of the AMOC (Caesar et al. 2018; Keil et al. 2020; Drijfhout et al. 2012).

However, the role of the AMOC decline in the uncertainty of the Euro-Atlantic atmospheric circulation remains unclear, as future projections mix the signals of the AMOC weakening with those to anthropogenic forcing (e.g. Bonnet et al., 2021). Inferring the climate response from pre-industrial water hosing experiments alone is also problematic as a recent study suggests that the impacts of an AMOC slowdown depend on the background climate (Bellomo and Mehling 2024). Further, the impacts of an AMOC decline on climate variability at daily timescales has only been analysed in two single model studies (Bellomo et al. 2023; Meccia et al. 2023). To address the aforementioned research gaps, we analyse the output of a large set of climate simulations from the CMIP6 archive under different forcings (Eyring et al. 2016) adopting a storyline perspective (Shepherd et al. 2018). Storylines here refer to climate trajectories characterized by either a stronger or weaker decline in the AMOC. By comparing these trajectories, we explore future climate uncertainty stemming from differences in oceanic responses among models. Furthermore, we complement the analysis with an ad-hoc experiment performed with state-of-art EC-Earth3 climate model (Döscher et al. 2022). This approach allows us to investigate mechanisms of response to an AMOC decline and separate them from those due to increased CO2 in a controlled experimental setup, while we are able to generalise our results stemming from the CMIP6 ensemble analysis. In particular, we focus on changes at subseasonal timescales using the framework of the Weather Regimes, extending prior work that focused on impacts of AMOC on the mean climate state only.

2 Data and methods

2.1 CIMP6 data

We analyse a set of climate model simulations participating in the sixth Coupled Model Intercomparison Project (CMIP6) forced with both realistic and idealised radiative forcing experiments (Eyring et al. 2016). We examine 22 SSP5−8.5 simulations, 19 SSP2−4.5 simulations, and 14 abrupt-4XCO2 simulations. The SSPs (Shared Socioeconomic Pathways) are climate change scenarios based on alternative pathways of emissions and land use changes during the 21st century, where the SSP5−8.5 represents the strongest forcing scenario, producing a radiative forcing of 8.5 W/m^2 in 2100, and SSP2−4.5 an intermediate forcing scenario, producing a radiative forcing of 4.5 W/m^2 in 2100 (O'Neill et al. 2016). The abrupt-4xCO2 is an idealised 150 years-experiment, where the CO2 concentration is abruptly increased to four times the preidustrial levels and maintained to this value. To assess changes in the atmospheric circulation, we compare the SSP experiments with the corresponding historical simulations, forced with radiative forcing estimated for the 1850–2014 period, and the abrupt-4XCO2 experiments with the piControl simulations, where the simulations are run in preindustrial conditions for 500 years without externally imposed anthropogenic forcing. For each model, we select only one ensemble member (r1i1p1f1 when available) in order to maximise the number of models included in the analysis, based on data availability. In fact, it has been suggested that the spread of atmospheric responses explained by the AMOC weakening is likely to be driven by differences in model formulations rather than by internal variability (Chemke et al. 2022). Table S1 (in the Supplementary Information) lists the models and corresponding ensemble members included in the analysis.

We analyse changes in temperature, ocean mixed layer depth, zonal wind, geopotential height and the storm track. To compute Euro-Atlantic Weather Regimes (hereafter, WRs), we use daily fields of geopotential height at 500 hPa. First, we interpolate all data to a common 2.5 × 2.5 grid using a bilinear interpolation. Since we are interested in large-scale patterns of atmospheric circulation, using a coarse grid does not influence our results. We analyse the Euro-Atlantic sector (30–90N°, -40–80°W) in the extended wintertime season (November through March,"NDJFM"), when the Northern Hemisphere mid-latitude atmospheric dynamical variability is largest. We use as reference period for the historical simulations the years 1950–2014 (65 years), and we compute future changes (with respect to the historical) taking the last 30 years of the century (2071–2100) from the SSPs scenarios. For preindustrial control we use as reference period the years from 50 to 199 (150 years), computing abrupt-4xCO2 changes from the preindustrial choosing the years from 90 to 139 (50 years). Using a longer period for the piControl does not affect the results.

2.2 The AMOC index and model classification

The AMOC strength index is computed as the maximum of the ocean meridional overturning stream-function below 500 m depth at 26.5°N. To isolate the atmospheric response to the AMOC decline in coupled atmosphere-ocean simulations, we take advantage of the large inter-model spread in AMOC weakening. Therefore, similarly to Bellomo et al. (2021) and Cerato et al. (2025), we split each ensemble in two groups based the projected AMOC index changes: Large-AMOC Decline group (LAD) and Small-AMOC Decline group (SAD). For each experiment, a model is classified as LAD if the AMOC index falls below the median of the distribution, otherwise it is classified as SAD. Table S1 shows the AMOC index change for each model and the corresponding classification. We analyse the different atmospheric response between the two groups, and interpret the difference as the effect of the AMOC weakening, when the difference is statistically significant (see Sect. 2.6).

2.3 Fixed-AMOC experiment

Since in the CMIP6 experiments described above the atmospheric response is both impacted directly, by changes in greenhouse gas concentration and other external forcings, and indirectly, by changes modulated through AMOC, we are not able to cleanly separate the pure AMOC influence on the atmosphere even when dividing models based on the AMOC decline, i.e., in SAD and LAD sub-ensembles. In fact, increasing greenhouse gases also cause the AMOC to decline. To address this issue, we further analyse an ad-hoc model experiment carried out with EC-Earth3 state-of-the-art climate model (Döscher et al. 2022), which participated in the CMIP6. We compare the EC-Earth3 abrupt-4xCO2 simulation from the CMIP6 archive, wherein the AMOC weakens in response to the imposed forcing (see Fig. S4), with an identical simulation, except that the strength of the AMOC is artificially maintained at the pre-industrial level despite the CO2 increase. In this stabilisation experiment, the AMOC strength is kept fixed by imposing a uniform positive virtual salinity flux (equivalent to + 0.6 Sv) poleward of 50°N in the Atlantic and Arctic Oceans (see Fig. S5). In describing the EC-Earth3 results, we will refer to this experiment as "Fixed AMOC", while to the abrupt-4xCO2 experiment as "Weakened AMOC". The difference in the atmospheric circulation response between the Weakened AMOC and the Fixed AMOC simulations can be formally attributed to the AMOC weakening, and is used to corroborate the findings of the multi-model CMIP6 analysis. For further details regarding the experimental design, we direct the reader to Bellomo and Mehling (2024) where these experiments are described.

2.4 Mean state response

For the CMIP6 models, the climatological response to AMOC weakening is defined for each experiment as the difference between the LAD and SAD ensemble mean:

$$\Delta X_{\mathrm{AMOC}} = \frac{1}{m}\sum_{i=1}^{m}\frac{\Delta X_{\mathrm{LAD}_i}}{\Delta \mathrm{GSAT}_i} - \frac{1}{n}\sum_{i=1}^{n}\frac{\Delta X_{\mathrm{SAD}_i}}{\Delta \mathrm{GSAT}_i} \tag{1}$$

where ΔX is the climatological change of a variable in each grid-point, which is divided by ΔGSAT, i.e., the change in the Global Surface Air Temperature. Normalising the change by the global mean temperature change reduces the influence of different climate model sensitivities on our estimates of AMOC impacts. However, we note that models with higher or lower climate sensitivity do not systematically fall into the same categories as the LAD and SAD groups—that is, changes in GSAT (ΔGSAT) are not correlated with changes in AMOC strength (ΔAMOC) (not shown). Therefore, differences in climate sensitivity across models are unlikely to be a primary driver of the group separation or to affect our main conclusions.

2.5 Euro-Atlantic Weather Regimes

The WRs framework allows us to classify each daily circulation pattern into a reduced number of recurrent and quasi-stationary atmospheric states, which are interpreted as dynamically stable equilibria of the atmosphere in non-linear system theory (Michelangeli et al. 1995; Hannachi et al. 2017; Hochman et al. 2021). Despite the exact number of the preferred atmospheric configurations is a matter of debate (Hannachi et al. 2017; Christiansen 2007; Dorrington et al. 2022a), most studies consider four wintertime Euro-Atlantic WRs: the positive phase of the North Atlantic Oscillation (NAO+), the Scandinavian Blocking (SBL), the Atlantic Ridge (AR) and the negative phase of the North Atlantic Oscillation (NAO−) (Michelangeli et al. 1995; Strommen et al. 2019; Fabiano et al. 2020; Wiel et al. 2019). In agreement with seminal studies (Palmer 1999; Corti et al. 1999), and with more recent analyses (Dorrington et al. 2022b) we analyse the WRs response to an external forcing as a change in their frequency of occurrence rather than changes in the patterns. Therefore, following the method outlined in Fabiano et al. (2020), we compute the Euro-Atlantic WRs from a reference dataset, i.e. ERA5 reanalysis (Hersbach et al. 2020), and we use these patterns as a common reference for all models simulations. By doing so, we do not consider changes due to model biases and their different representations of regimes' spatial patterns.

ERA5 WRs are computed from daily 500 hPa geopotential height fields ($zg500$). First, we detrend the $zg500$ time series to remove the effect of the mean thermal expansion of the atmosphere due to global warming. In particular, we remove the linear fit to the area-weighted average Euro-Atlantic time series. Secondly, for each grid point we remove the smoothed daily seasonal cycle (20 days running mean) to obtain geopotential height anomalies ($zg500'$), which represent large-scale daily atmospheric variability. As in previous studies (e.g. Michelangeli et al., 1995; Cassou, 2008; Dawson et al., 2012), we compute WRs applying a K-means clustering on the leading Principal Components (PCs). Specifically, using the *eofs* Python package (Dawson 2016), we project the anomalies onto the phase space spanned by the first four leading EOFs, which explain ∼ 53.3% of the variance (hereafter "reference phase space"), reducing dimensionality and the effect of atmospheric noise. Negligible changes are found when increasing the number of EOFs used to define the reference phase space. Finally, we perform K-means clustering on the resulting PCs, setting a-priori the number of clusters to be four. The ERA5 WRs are the centroids of each cluster, shown in Fig. 5 as the composites of the anomalies assigned to each centroid.

We use these patterns as reference to analyse the change in WRs frequency and persistence in climate model experiments. The simulated $zg500$ are processed analogously to ERA5. However, following Fabiano et al. (2021), to obtain $zg500'$ from the SSP2−4.5, SSP5−8.5 and abrupt-4XCO2 we remove the smoothed daily seasonal cycle (20 days) computed in the corresponding historical or piControl. As a result, we preserve in the time series the change in the mean geopotential height, that is part of the signal in which we are interested in. Thereafter, the simulated $zg500'$ from all the experiments are projected onto the reference phase space, producing a set of pseudo-PCs (not being projected onto each model's EOFs, they cannot be properly termed PCs). The classification is finally achieved based on the minimum Euclidean distance between the pseudo-PCs and the reference centroids. Importantly, before the classification, we add a fifth centroid at the origin of the reference phase space, to represent climatological conditions, as recommended by Lee et al. (2023). The fifth centroid, named "No Regime", allows for a more realistic classification of days when the anomalies are negligible and do not resemble any of the other four centroid patterns. At this point, the mean frequency of each WR is defined as the percentage of days assigned to a centroid, while the mean persistence is defined as the average duration of a single event. For the calculation of the mean persistence, the definition of the duration of an event (i.e., number of consecutive days in which the atmosphere is classified as a specific regime) is adjusted to allow for one-day deviations from the regime state; therefore, a regime event ends only when two consecutive days are assigned to a different regime.

2.6 Statistical tests

To ensure the validity of the following results we rely on statistical tests. Specifically, when assessing whether the difference between two distributions is significant (e.g., the difference in responses between the LAD and SAD model groups), we use a two-tailed Welch's t-test (Welch 1947) with a 95% confidence level. When explicitly evaluating the correlation between two variables across climate models, we apply a non-parametric bootstrap approach. In this method, model data are randomly shuffled 10^4 times, and the correlation is recalculated at each iteration (with the sample size equal to the number of models). The corresponding p-value is the proportion of bootstrap iterations in which the absolute value of the resampled correlation exceeds that of the original dataset. The caption of each figure specifies which statistical test has been applied to assess the significance of the results.

3 Results

3.1 The AMOC decline

The AMOC strength weakens in the three experiments, in agreement with previous studies (Weijer et al. 2020; Bellomo et al. 2021; Baker et al. 2023; Mecking and Drijfhout 2023). Figure 1 shows the time series of the AMOC strength anomaly in the three coordinated CMIP6 experiments. Following the applied forcing, in the SSP2–4.5 and SSP5–8.5 experiments the AMOC declines steadily, while in the abrupt-4xCO2 experiment the AMOC declines abruptly until it reaches a plateau, roughly after year 50 for all models. In some models the AMOC shows a recovery at the end of the abrupt-4xCO2 simulation. Compared to the reference climates, the AMOC weakening ranges approximately from -3Sv to -10Sv in the SSP2–4.5, from -4Sv to -13Sv in the SSP5–8.5, and from -3Sv to -14Sv in abrupt-4xCO2. The classification into LAD (Large-AMOC-Decline) and SAD (Small-AMOC-Decline) is indicated in the figure by red and blue lines, respectively.

3.2 Euro-Atlantic mean state response

In this section, we show the analysis conducted on the SSP5–8.5 simulations while a summary of the climatological response of the SSP2–4.5 and abrupt-4xCO2 experiments is given in the Supplementary Information, with similar results (Figs. S1 and S2). The impact of the AMOC weakening on the atmosphere is mediated by temperature anomalies at the interface between the ocean and the atmosphere. Therefore, we analyse changes in surface temperature that over the ocean coincides with the SST while over land corresponds to the temperature at the surface. We compute the normalised response (2071–2100 average minus 1950–2014 average) in the LAD and SAD groups (Fig. 2a–b), finding the minimum SST warming in the SPNA, the North Atlantic Warming Hole (NAWH) (e.g. Menary and Wood, 2018), more pronounced in the LAD models compared to the SAD models. The response to the AMOC weakening is the difference between the LAD and SAD responses (see Eq. 1), which is a relative cooling of the Euro-Atlantic region (Fig. 2c), consistent with a reduced northward ocean heat transport.

Furthermore, we analyse changes in Mixed Layer Depth (MLD), i.e. the deepest ocean depth affected by turbulent mixing, which is closely related to the AMOC deep convection (Fig. 2d–f). First, we note the difference in the historical

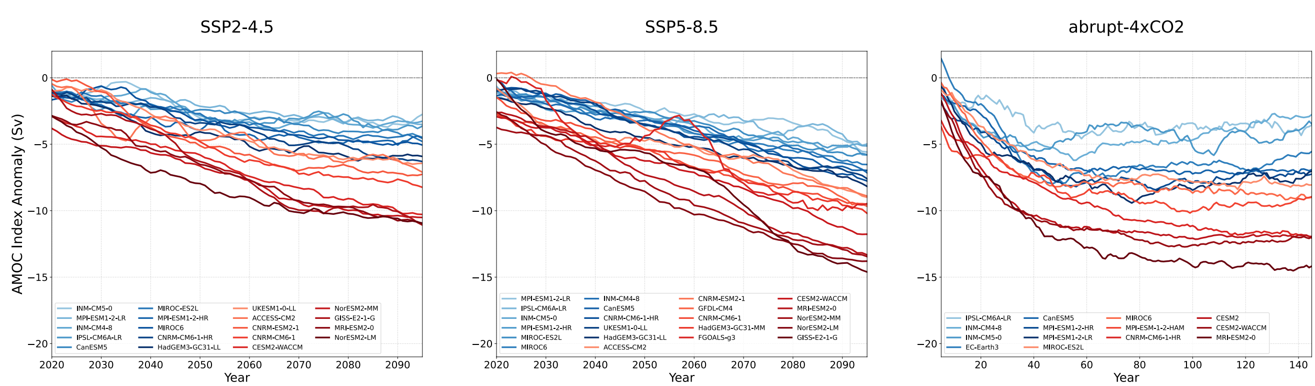

Fig. 1 Annual AMOC strength anomalies at 26.5N in SSP2–4.5 and SSP5–8.5 experiments computed with respect to the mean historical AMOC strength, and in the abrupt-4xCO2 experiment computed with respect to the mean AMOC strength in the piControl. Blue lines represent models in the Small AMOC decline group (SAD) while red lines models in the Large AMOC decline group (LAD). A 10-year moving average has been applied for better visualization

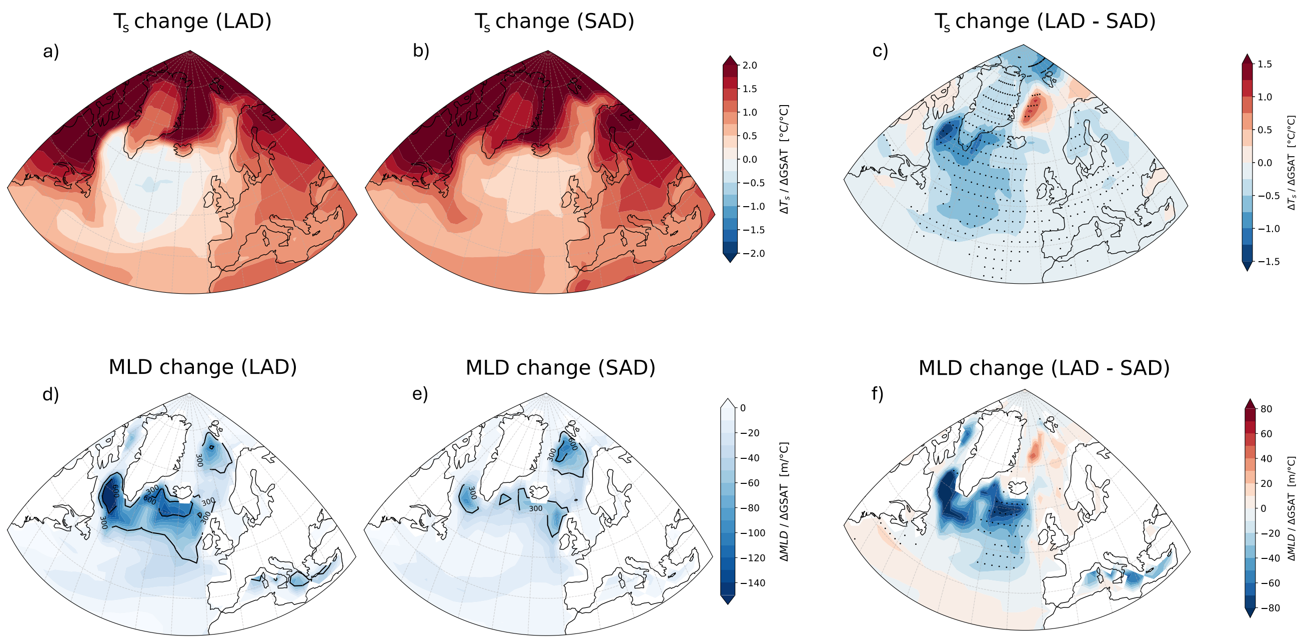

Fig. 2 Ensemble mean surface temperature change (SSP5−8.5) in LAD group (**a**), SAD group (**b**) and their difference (**c**), normalised by ΔGSAT. Stipplings in (**c**) represent statistical significance difference between SAD and LAD responses (two-tailed Welch t-test at 95% level). **d**–**f** The same for mixed layer depth is computed using fewer models based on data availability i.e. 10 models from the LAD group (HadGEM3-GC31-MM missing) and 6 models from SAD group (HadGEM3-GC31-LL, INM-CM4-8, INM-CM5-0 and MIROC-ES2L are missing). Superimposed contours in (**d**) and (**e**) represent the climatological mixed layer depth ensemble mean for LAD and SAD models, respectively

deep convection between the LAD and SAD ensemble means (superimposed contours in Fig. 2d–e). In the LAD models the MLD is generally deeper in the Labrador and Irminger seas, whereas in the SAD models the region of strongest convection is the GIN seas. The MLD response (Fig. 2f) shows a greater reduction in deep convection in the LAD models, especially in the Labrador sea and Irminger sea (where it is statistically significant). This is in agreement with the mechanism proposed by Lin et al. (2023), whereby a weaker Labrador sea stratification in the climatology leads to a stronger AMOC decline with an increased CO2 concentration, explaining the correlation between the AMOC mean state with its projected weakening. The LAD group also show a smaller reduction in deep convection in the GIN seas compared to SAD models under the SSP5−8.5, due to a smaller convection already in the historical period. Remarkably, the MLD response pattern is largely consistent with the temperature response pattern (Fig. 2c), demonstrating the direct link between a greater AMOC decline and the relatively cold surface temperature anomalies.

These anomalies propagate up into the atmospheric column influencing the atmospheric thermal structure of the Euro-Atlantic sector. We compute the normalised zonally averaged air temperature response difference between LAD and SAD models (Fig. 3a), finding a general cooling of the Euro-Atlantic atmosphere and, interestingly, a significant

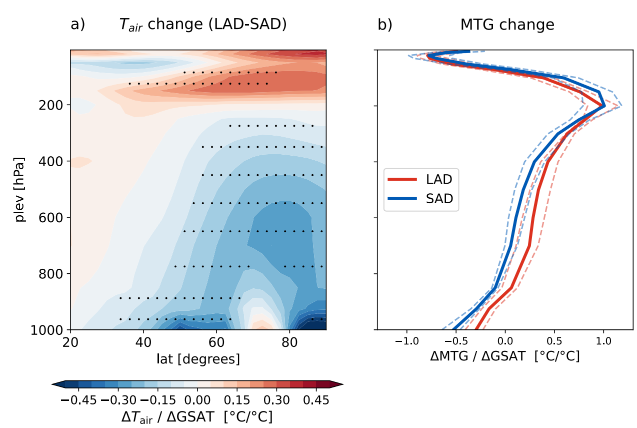

Fig. 3 **a** Ensemble mean zonally averaged air temperature response difference between LAD and SAD groups (SSP5−8.5) normalized by ΔGSAT. Stippling indicates the statistical significance of the difference between LAD and SAD (two-tailed Welch t-test at 95% confidence level). **b** Meridional Temperature Gradient (MTG) change in LAD and SAD groups. MTG is computed as the difference between zonally averaged temperature in the 20°N-40°N and 50°N-70°N latitudinal bands for each atmospheric pressure level. Solid lines represent the ensemble mean while dashed lines represent the 25th and 75th percentiles of the LAD and SAD distributions

warming in the stratosphere. Consistent with the reduced tropospheric warming, LAD models show a relative increase of the Meridional Temperature Gradient (MTG) (Fig. 3b), which is quantified as the difference between zonally averaged temperature in the 20°N-40°N and 50°N-70°N latitudinal bands for each atmospheric pressure level. In the lower-troposphere the MTG is projected to decrease in most models. However, in LAD models the MTG weakening is partly counteracted by the AMOC decline, which is also consistent with a reduced Arctic Amplification, as shown in Fig. 3a. The MTG is the source of the atmospheric baroclinicity that fuels storms formation, directly related to the speed of mid-latitude jet through the thermal wind balance. Therefore, we expect significant differences in the projected atmospheric circulation between LAD and SAD models.

In Fig. 4 we show the response of the mean westerly flow, the storm track and the 500 hPa geopotential height. We find a significant strenghtening of the 250 hPa westerly wind in LAD compared to SAD models. The mid-latitude jet stream is therefore intensified and elongated towards Europe (Fig. 4c). The same pattern is found at 850hPa (not shown), suggesting a barotropic response of the flow to the AMOC weakening. Similarly, the North Atlantic storm track is projected to intensify to a greater extent in LAD models, especially in its downstream flank, in the center of action of the North Atlantic Oscillation (NAO) (Fig. 4f). The mean geopotential height difference between the LAD and SAD ensemble means features negative anomalies over the Northern North Atlantic and positive anomalies over the Mediterranean, resembling the positive phase of the NAO (Fig. 4i).

3.3 Change in frequency and persistence of Weather Regimes

The ERA5 winter time WRs are shown in Fig. 5: the two phases of the North Atlantic Oscillation (NAO+, NAO−), the Scandinavian blocking (SBL) and the Atlantic Ridge (AR). These patterns are used as reference for the computation of the WRs frequency (percentage of days assigned to each regime) and persistence (average duration of a regime event) in the climate change simulations. Superimposed contours in Fig. 5 are the composites of the low-pass filtered low-level zonal wind (average over 700–850 hPa pressure levels), indicating the position of the low-level (eddy-driven) jet stream. In the reanalysis, the most frequent regime is the NAO+ (25.9% of the days), while the most persistent

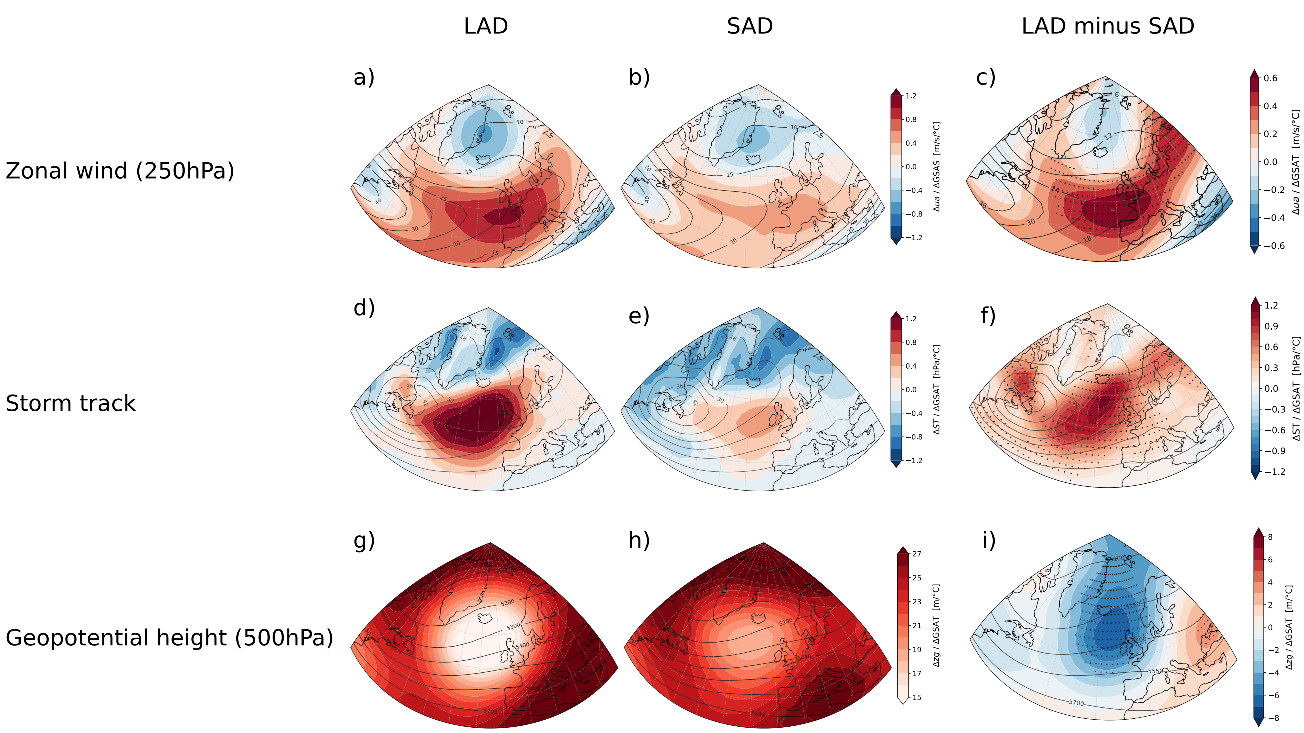

Fig. 4 Response of the mean atmospheric circulation to the AMOC decline (zonal wind at 250 hPa, North Atlantic storm track, geopotential height at 500hPa) in the SSP5−8.5. The first two columns represent the normalised ensemble mean response of the LAD and SAD groups, respectively. Shadings in the third column represent their difference, while stippling the statistical significance of the difference between LAD and SAD groups (two-tailed Welch t-test at 95% confidence level). The storm track is computed as the band-pass filtered (2–6 days) variance of daily sea level pressure anomalies. For the storm track computation the GISS-E2-1-G, FGOALS-g3 models were not available. Contours in the figures represent the ensemble mean climatology

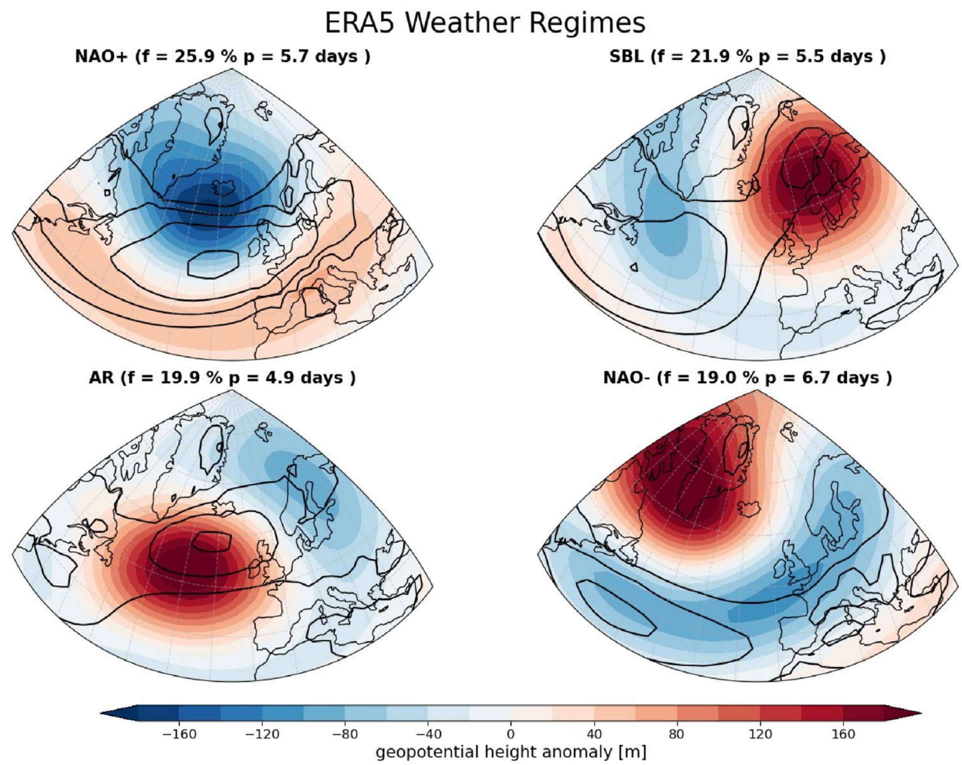

Fig. 5 Wintertime Euro-Atlantic Weather Regimes in the ERA5 reanalysis (1950–2014). The assignement of the daily anomalies is performed after the addition of the "No Regime" state based on the minimum Euclidean distance to the centroids in the reference phase space (see Methods). Round brackets indicate the mean frequency (f), computed as the average number of days assigned to a regime, and the mean persistence (p), computed as the average duration of an event allowing for 1-day deviations to other regimes. Superimposed contours are the composites of the low-pass filtered (10-days) low-level (700-850hPa average) daily zonal wind. Contours start from 4 up to 16 m/s (every 4 m/s)

is the NAO− (average event is 6.9 days). The jet composites show that out of the four regimes, three are "blocked". The Scandinavian Blocking is characterised by a blocking located over Scandinavia and the British Isles and by a tilted eddy-driven jet from South-West to North-East. The Atlantic Ridge is blocked over the Atlantic and associated with a northern position of the jet. The NAO− is characterised by a blocking over Greenland which pushes the jet south. Finally, the positive phase of the NAO is "unblocked", and is associated with a central position of the jet close to its climatology. Therefore, variations in WRs statistics are dynamically related to the variability of the jet, which are among the primary factors influencing the winter-time Euro-Atlantic climate and extreme weather conditions (Dorrington et al. 2022a; Barnes and Polvani 2013).

Figure 6 displays changes in the distributions of the WRs frequency across the three experiments. Examining all models (purple bars), reveals a projected increase in NAO+ frequency, alongside a general decrease in SBL and AR frequencies. This response aligns with Fabiano et al. (2021) for the SSPs experiments and with Dorrington et al. (2022b), who analysing geopotential-jet regimes show that zonal flow conditions become more prevalent at the expense of AR and SBL. Thus, in a warmer climate, models predict an increased occurrence of NAO+ at the expense of SBL and AR. Interestingly, despite a stronger forcing, the abrupt-4xCO2 distributions does not consistently show a stronger WR frequency response. Moreover, the abrupt-4xCO2 generally exhibits a larger inter-model spread in the WRs response, as for the AMOC index (Fig. 1). When splitting the distributions into the LAD and SAD groups (red and blue bars respectively), the frequency of the NAO+ regime exhibits a net increase in LAD models which is much reduced in SAD models, especially in SSP2−4.5 and SSP5−8.5 where the difference between LAD and SAD distributions is statistically significant (red stars in the figure). Thus, the projected increase in the frequency of the NAO+ regime in the full ensemble mostly originates from models in which the AMOC declines more. Conversely, the other three frequencies do not show a clear relation with the AMOC decline. Although generally AR and SBL frequencies decrease more sharply in LAD models than in SAD models, the signal is not statistically significant. The NAO− is not influenced by the AMOC decline, since the frequency response is similar between LAD and SAD groups. Finally, we observe a reduced occurrence of "No Regime" days in LAD compared to SAD models, although the difference is not statistically significant (Fig. S4). A similar but noisier pattern is found for persistence, as shown in the Supplementary Information (FigS3). However, differently from the frequency response, the NAO+ persistence response differs between the LAD and SAD groups significantly (95% confidence level) in abrupt-4xCO2 experiment, and not in the the SSP2−4.5 and SSP5−8.5.

In summary, we find that the NAO+ regime is sensitive to AMOC decline. This is explicitly illustrated in

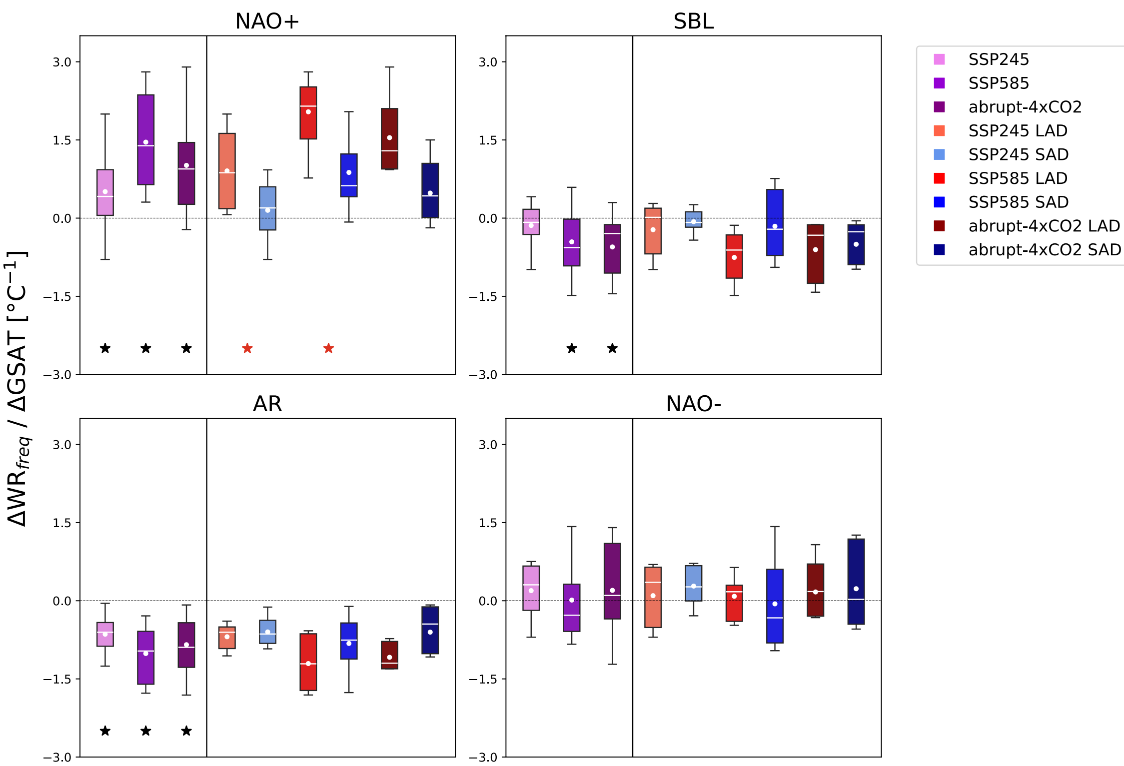

Fig. 6 Normalised response of WRs frequency in the three experiments. The boxes represent the interquartile range (from the 25th to the 75th percentile), with the white line and dot indicating the median and the mean, respectively. The whiskers extend to the 5th and 95th percentiles. Black stars denote that distributions of changes are significantly different from zero (two-tailed one-sample t-test, 95% confidence level). Red stars indicate significant differences between the LAD and SAD distributions (two-tailed Welch's t-test, 95% confidence level)

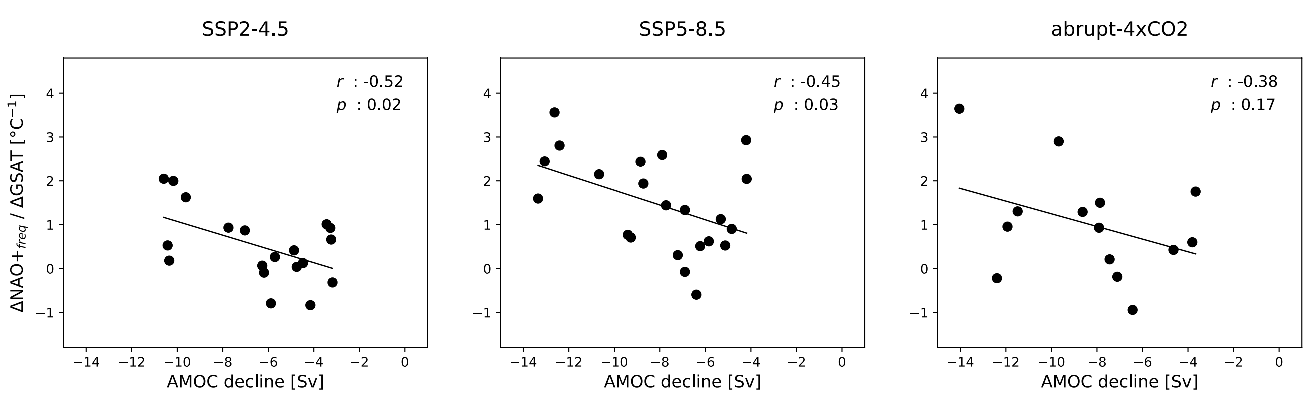

Fig. 7 Scatterplots of normalised NAO+ frequency changes against the projected AMOC weakening in the three experiments. The black solid line represents the linear regression model estimating the correlation between the two variables, expressed with the *r* coefficient (Pearson correlation). The p-value is computed with bootstrap as indicated in the Methods (Sect. 2.6)

Fig. 7, where the scatterplots reveals a significant correlation between the AMOC decline in the SSP2−4.5 and SSP5−8.5 (r = −0.52 and −0.45, respectively). On average, a greater AMOC weakening corresponds to a greater NAO+ frequency response. Interestingly, the correlation is weaker in the abrupt-4xCO2 experiment. While several processes contribute to the evolution of the Euro-Atlantic atmospheric circulation (e.g. Shaw et al., 2016), we argue that the weakening of AMOC accounts for a significant portion of model uncertainty in future projections at the sub-seasonal scale.

3.4 Relation between Weather Regimes and mean state changes

Changes in the WRs statistics are intrinsically linked with changes in the climatological circulation. In particular, we explore the connection between the mean *zg*500 response and the change in NAO+ frequency. In Fig. 8, the x-axis represents a coefficient obtained by projecting the simulated mean *zg*500 change onto the NAO+ pattern derived from ERA5. This coefficient quantifies the similarity between the simulated mean *zg*500 response to the NAO+ spatial structure. Across simulations, we find a strong positive correlation between this coefficient and the change in NAO+ frequency, indicating that the more the *zg*500 response resembles the NAO+ pattern, the greater the increase in NAO+ occurrence.

Therefore, changes in the WRs are consistent with the influence of the AMOC on the mean geopotential height. The AMOC associated temperature anomalies enhance atmospheric baroclinicity (Figs. 2, 3), which leads to an intensification of the North Atlantic jet (Fig. 4c). According to the geostrophic balance, this intensification projects onto a mean geopotential height anomaly pattern resembling the positive phase of the NAO (Fig. 4i). From a WRs perspective, this translates into an increased occurrence of the NAO+ regime (Figs. 6, 7).

3.5 Fixed AMOC experiment

Analysis of CMIP6 simulations indicates that the NAO positive phase is influenced by the reduction in the AMOC strength. However, concurrent increases in greenhouse gas concentrations can also have direct, atmospheric impacts on WRs, complicating the separation of anthropogenic and AMOC-driven effects. Using the EC-Earth3 model, we corroborate the above findings with an ad-hoc model experiment in which the AMOC strength is artificially controlled while forcing the model with abrupt-4xCO2 (as detailed in the Methods, see also Fig. S5). Figure 9 illustrates the mean response differences between the Weakened AMOC (abrupt-4xCO2) and Fixed AMOC experiments. The results are broadly consistent with the CMIP6 multi-model analysis: A weakened AMOC leads to reduced mixed layer depth (MLD; Fig. 9b), cooling over the North Atlantic (Fig. 9a), and an increased meridional temperature gradient (MTG; Fig. 9c). The jet stream intensifies and extends eastward towards Europe (Fig. 9d), accompanied by an intensified storm track, particularly on its northeastern flank (Fig. 9e). The geopotential height responds with a negative anomaly near the NAO's center of action (Fig. 9f).

The response of WRs is also consistent with the CMIP6 analysis. Figure 10 depicts time series of WRs seasonal mean frequencies in the Weakened and Fixed AMOC experiments. Note that EC-Earth3 is one of the few models in which the 4xCO2 forcing results in a decreased NAO+ frequency (-6%) compared to the preindustrial climate. However, by stabilising the AMOC, the NAO+ frequency decreases significantly more (−12.5%), confirming the AMOC weakening to increase the NAO+ occurrence. The net effect of AMOC weakening is also a reduction in SBL, similar to the multi-model analysis. However, unlike in that case, the reduction observed here is statistically significant.

4 Summary and discussion

The presence of multiple competing drivers of large-scale atmospheric circulation changes makes future projections uncertain in the Euro-Atlantic, undermining our confidence about the impacts of climate change in Europe. In this paper, we investigate the role of the AMOC, which is robustly projected to weaken in future climate projections. We analyse

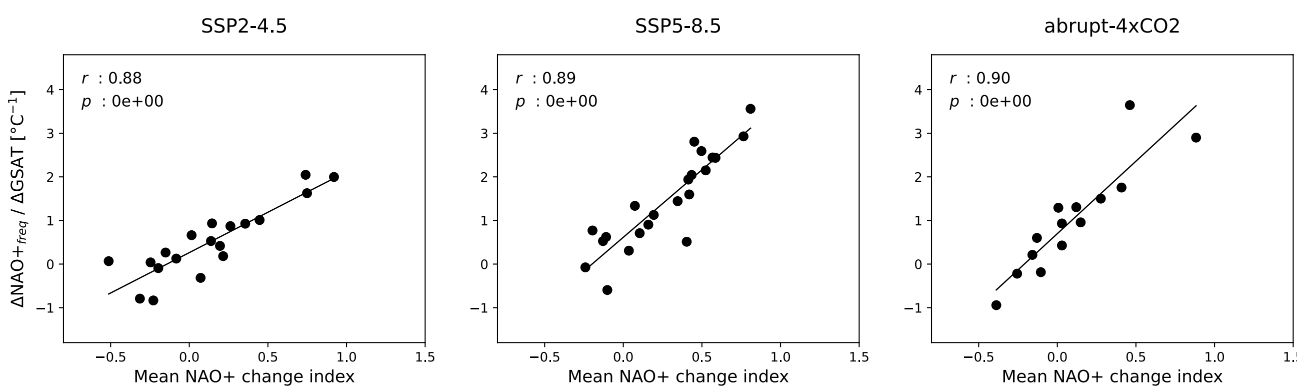

Fig. 8 Mean 500 hPa geopotential height response (*zg*500) against NAO+ regime frequency change in the three experiments. The "Mean NAO+ change index" is a spatial correlation coefficient obtained by projecting *zg*500 onto the NAO+ pattern. Black solid lines represent the linear regression models estimating the correlation between the two variables, expressed with the *r* coefficient (Pearson correlation). The p-value is computed with bootstrap as indicated in the Methods (Sect. 2.6)

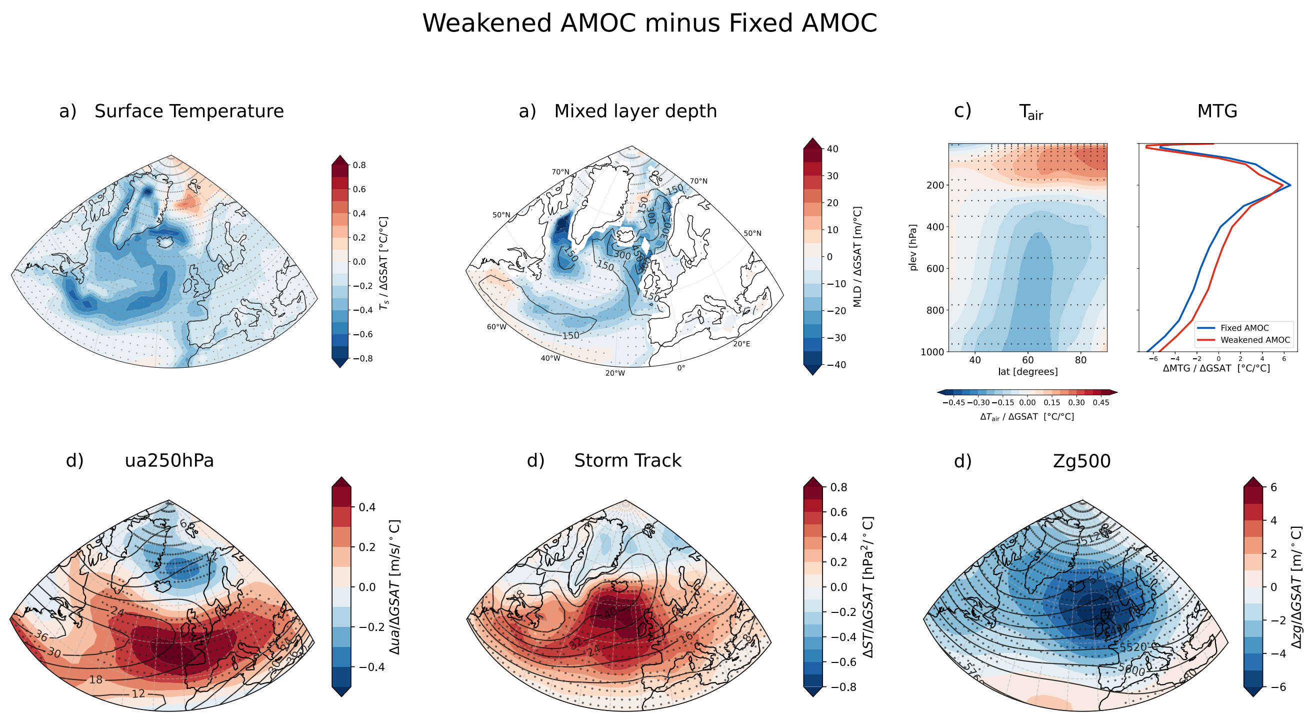

Fig. 9 Climatological response in the EC-Earth3 Weakened AMOC experiments compared to the Fixed AMOC experiment (normalised by ΔGSAT) in Surface Temperature (**a**), Mixed Layer Depth (**b**), Zonal mean air temperature and Meridional Temperature Gradient (**c**), zonal wind at 250 hPa (**d**), storm track (**e**) and geopotential height at 500 hPa (**f**). Stipplings indicate where the signal is statistically significant. The statistical significance is computed with a two-tailed Welch t-test at 95% confidence level between seasonal mean values in the Weakened AMOC and Fixed AMOC experiments for each grid-point

three sets of CMIP6 simulations with a storyline approach (Shepherd et al. 2018), comparing the atmospheric response between models in which the AMOC declines more (LAD) and models in which the AMOC declines less (SAD). We further analyse a Fixed-AMOC experiment carried out with EC-Earth3 to isolate the response of the AMOC decline in a warmer climate.

The two complementary analyses provide a consistent picture. A larger AMOC decline is associated with a reduced warming of the Euro-Atlantic, especially in the SPNA where a larger NAWH develops (Fig. 2c). As a result, we observe a relatively smaller reduction of the zonally averaged meridional temperature gradient (MTG) in the troposphere (Figs. 3, Fig. 9c). The wintertime mean atmospheric circulation responds with a strengthening of the westerly flow, which is more zonal and elongated towards Europe (Figs. 4c, 9d), an intensification of the storm track in the eastern North-Atlantic (Figs. 4f, 9e), and geopotential height pattern that resembles the positive phase of the North Atlantic Oscillation (Figs. 4i and 9f). These impacts are broadly consistent with prior water-hosing experiments based on preindustrial climates (Bellomo et al. 2023; Jackson et al. 2015; Brayshaw et al. 2009) and with fixed-AMOC experiments based on historical and RCP−8.5 forcings (Liu et al. 2020; Lee et al. 2024; Mimi and Liu 2024). Additionally, these results are consistent with Gervais et al. (2019), who isolated the effects of an imposed a NAWH under the RCP−8.5 forcing.

Building on the previous studies, we further analyse changes in the atmospheric circulation at sub-seasonal time scales using the concept of Weather Regimes. We find a significant sensitivity of the NAO+ regime occurrence to the magnitude of the AMOC weakening in the SSP2−4.5 and SSP5−8.5 ensembles, as well as in the Fixed-AMOC experiment. Across these simulations, the frequency of the NAO+ regime generally increases as the AMOC weakens (Figs. 7, 10). In contrast, the signal is weaker in the abrupt-4xCO2 ensemble. Consistent with a more zonal, "unblocked" flow, the occurrance of SBL and AR are reduced. However, there is no model agreement about which of these two regimes is the most affected by the increased NAO+ occurrence, since in SSP2−4.5, SSP5−8.5 and abrupt-4xCO2 ensembles their decreasing occurrence is not significant. Interestingly, the blocking over Greenland (NAO−) does not appear to be affected by the AMOC decline (Figs. 6, 10). This particular aspect contrasts with the findings of Bellomo et al. (2023), who conducted water-hosing experiment using EC-Earth3. However, is important to note that our study assesses the impacts of AMOC weakening in a warmer climate. Additionally, the inclusion of the "No Regime" state in our WRs analysis allows for an increase in the frequency

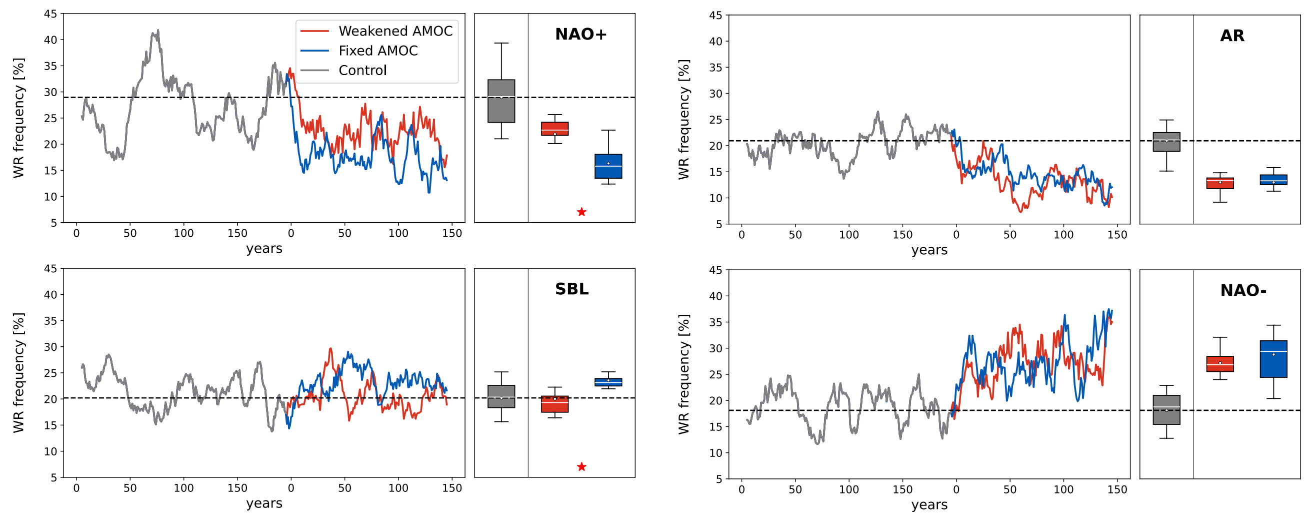

Fig. 10 On the left hand side of each panel the time series of seasonal mean WRs' frequency in the Weakened and Fixed AMOC experiments. Grey lines indicate the last 200 years of the piControl experiment, while red and blue lines the 150-years Weakened and Fixed AMOC experiments, respectively. A 10-year running average smoothing is applied for better visualization. On the right side of each panel boxplots of 10-year mean frequencies in the experiments. Red stars indicate significance difference between the two distributions at the 95% confidence level (Welch two-tailed t-test)

or persistence of a particular regime without necessarily decreasing the occurrence of others, providing a more realistic identification of the forced signal.

Mechanistically, we hypothesise that atmospheric impacts of the AMOC weakening are driven by thermodynamic effects. The reduced AMOC heat convergence, indicated by the shallowing of the Mixed Layer Depth (Figs. 2f and 9b), drives the development of the NAWH (Keil et al. 2020; Caesar et al. 2018; Drijfhout et al. 2012), which is located where the deep convection occurs in the simulations. In the LAD group the climatological deep convection occurs mainly in the Labrador and Irminger Seas, where the Mixed Layer Depth is deeper compared to the SAD group in all the experiments we analysed (Figs. 2f and S1) and where in future projections a deeper NAWH appears. These temperature anomalies act to increase the already present SST gradient in the SPNA, resulting into an increased low-level atmospheric baroclinicity, which enhances the eddy activity reinforcing the eddy-driven-jet and the storm track. At the upper tropospheric levels, the thermal wind balance explains the intensification of the mean westerly flow as a consequence of a relative increase in the meridional temperature MTG. Consistent with geostrophic balance, this projects onto a geopotential height response which resembles the NAO+ pattern (see Figs. 4i, 9i and the schematics in Fig. 6 of Gervais et al., 2019), which from a Weather Regime perspective translates into an increased NAO+ occurrence.

One limitation of this study is that it does not explicitly account for internal variability in the Atlantic Ocean, which can significantly influence the atmospheric response simulated by climate models (Bonnet et al. 2021). Furthermore, our findings show some sensitivity to the specific methodology used to compute the AMOC index. For instance, using 45°N instead of 26.5°N as the reference latitude, or expressing AMOC decline in percentage rather than absolute terms, tends to reduce the statistical significance of the results, but does not change the main conclusions. Lastly, the interplay between AMOC decline and other potential drivers of circulation changes remains an open question and deserves further investigation. Our analysis reveals a significant correlation between AMOC weakening and Arctic Amplification, as seen in the zonal mean temperature profile. In SSP5−8.5 (Fig. 3) and SSP2−4.5 (Fig. S1), models with the strongest AMOC weakening tend to exhibit reduced Arctic Amplification. Similarly, in the EC-Earth3 experiment, AMOC weakening offsets Arctic warming (Fig. 9c), in agreement with Lee et al. (2024) and Liu and Fedorov (2022). This connection is further supported by previous studies identifying a negative NAO response to Arctic sea ice loss (Sun et al. 2022; Delhaye et al. 2023), which is of opposite sign to the positive NAO response given by the AMOC weakening. However, interestingly, the relation between AMOC and Arctic Amplification does not hold in the abrupt-4xCO2 ensemble, where the LAD group experiences greater Arctic warming (Fig. S1). This might suggests the relation to be model-dependent, and could contribute to the weaker circulation response seen in the abrupt-4xCO2 ensemble in both mean circulation (Fig. S2) and WRs analysis (Fig. 6). However, in all the experiments analysed here, the low-level MTG increases with the weakening of the AMOC (Fig. 3, Figs. 9c, S1), partially compensating for the reduction due to the Arctic Amplification, thus favoring the Upper-Tropospheric-Warming in the tug-of-war that determines the evolution of the circulation in the Euro-Atlantic (Shaw et al. 2016; Peings et al. 2018).

Overall, the key finding of this work is that uncertainty in the response of the large-scale Euro-Atlantic atmospheric circulation is linked to the inter-model spread in the AMOC decline, also at sub seasonal timescales. In Fig. 6 we show that the multi-model mean increase of NAO+ frequency is mainly driven by LAD models, indicating the importance of the AMOC weakening for this emerging impact in climate projections. The increase in NAO+ conditions correspond to a more frequent central position of the jet stream (Madonna et al. 2017) consistent with reduced variability in its daily latitudinal shifts (Barnes and Polvani 2013), and the projected reduction in atmospheric blocking frequency (Davini and D'Andrea 2020). Reducing the uncertainty related to the AMOC weakening is therefore essential for improving projections of climate change impacts in Europe. One important step towards this goal is enhancing the density and resolution of ocean circulation observational data. Another promising approach is identifying relationships between the current state of the climate and its predicted response in model simulations, commonly referred to as emergent constraints (e.g., Hall et al., 2019). In this context, our analysis of mean state differences in the deep convection region (Fig. 2) offers valuable insights into constraining the future AMOC decline.

Supplementary Information The online version contains supplementary material available at https://doi.org/10.1007/s00382-025-07747-z.

Acknowledgements This paper and related research have been conducted during and with the support of the Italian inter-university PhD course in sustainable development and climate change (link: www.phd-sdc.it). We acknowledge the Coupled Modelling Working Group of the World Climate Research Programme for overseeing CMIP, the climate modeling groups for producing the model outputs, and the Earth System Grid Federation (ESGF) for enabling public access to these data. The EC-Earth3 simulations shown in this work were carried out at ECMWF under the special projects SPITBELL, SPITMEHL and SPITVACC. K.B. acknowledge "The Geosciences for Sustainable Development" project (Budget Ministero dell'Università e della Ricerca–Dipartimenti di Eccellenza 2023–2027 C93C23002690001).

Author Contributions A.V.V. and K.B. conceived and designed the study. The data collection and analysis was carried out by A.V.V., with the contribution of all the authors, in particular F.F. for the analysis of Weather Regimes. The manuscript was written by A.V.V. and K.B., with contributions from all co-authors. All authors read and approved the final manuscript.

Funding This study was carried out within the RETURN Extended Partnership and received funding from the European Union Next-GenerationEU (National Recovery and Resilience Plan NRRP, Mission 4, Component 2, Investment 1.3 D.D. 1243 2/8/2022, PE0000005).

Data Availability The CMIP6 model output data are publicly available at https://esgf-metagrid.cloud.dkrz.de/search/cmip6-dkrz/. The EC-Earth3 experiment data can be requested by writing to K.B.. The code for reproducing the figures can be requested by writing to the corresponding author.

Declarations

Conflict of interest The authors declare that they have no relevant financial or non-financial interests to disclose.

References

Armstrong McKay DI, Staal A, Abrams JF, Winkelmann R, Sakschewski B, Loriani S, Fetzer I, Cornell SE, Rockström J, Lenton TM (2022) Exceeding 1.5°C global warming could trigger multiple climate tipping points. *Science*, 377(6611):eabn7950. Publisher: American Association for the Advancement of Science

Baker JA, Bell MJ, Jackson LC, Renshaw R, Vallis GK, Watson AJ, Wood RA (2023) Overturning Pathways Control AMOC Weakening in CMIP6 Models. Geophys Res Lett, 50(14):e2023GL103381. _eprint: https://onlinelibrary.wiley.com/doi/pdf/10.1029/2023GL103381

Barnes EA, Polvani L (2013) Response of the Midlatitude jets, and of their variability, to increased greenhouse Gases in the CMIP5 models. J Clim, 26(18):7117–7135. Publisher: American Meteorological Society Section: Journal of Climate

Barnes EA, Screen JA (2015) The impact of Arctic warming on the midlatitude jet-stream: Can it? Has it? Will it? WIREs Clim Change 6(3):277–286

Bellomo K, Angeloni M, Corti S, von Hardenberg J (2021) Future climate change shaped by inter-model differences in Atlantic meridional overturning circulation response. Nat Commun 12(1):3659

Bellomo K, Meccia VL, D'Agostino R, Fabiano F, Larson SM, Hardenberg Jv, Corti S (2023) Impacts of a weakened AMOC on precipitation over the Euro-Atlantic region in the EC-Earth3 climate model. *Climate Dynamics*

Bellomo K, Mehling O (2024) Impacts and State-Dependence of AMOC Weakening in a Warming Climate. Geophys Res Lett, 51(10):e2023GL107624. _eprint: https://onlinelibrary.wiley.com/doi/pdf/10.1029/2023GL107624

Bonnet R, Swingedouw D, Gastineau G, Boucher O, Deshayes J, Hourdin F, Mignot J, Servonnat J, Sima A (2021) Increased risk of near term global warming due to a recent AMOC weakening. Nat Commun, 12(1):6108. Publisher: Nature Publishing Group

Borchert LF, Müller WA, Baehr J (2018) Atlantic Ocean heat transport influences interannual-to-decadal surface temperature predictability in the North Atlantic region. Journal of Climate, 31(17):6763–6782. Publisher: American Meteorological Society Section: Journal of Climate

Brayshaw DJ, Woollings T, Vellinga M (2009) Tropical and extratropical responses of the North Atlantic atmospheric circulation to a sustained weakening of the MOC. J Clim 22(11):3146–3155

Bryden HL, King BA, McCarthy GD, McDonagh EL (2014) Impact of a 30% reduction in Atlantic meridional overturning during 2009 –2010. Ocean Sci, 10(4):683–691. Publisher: Copernicus GmbH

Buckley MW, Marshall J (2016) Observations, inferences, and mechanisms of the Atlantic Meridional Overturning Circulation: A review. Rev Geophys, 54(1):5–63. _eprint: https://onlinelibrary.wiley.com/doi/pdf/10.1002/2015RG000493

Butler AH, Thompson DWJ, Heikes R (2010) The steady-state atmospheric circulation response to climate change-like thermal forcings in a simple general circulation model. J Clim, 23(13):3474–3496. Publisher: American Meteorological Society Section: Journal of Climate

Caesar L, Rahmstorf S, Robinson A, Feulner G, Saba V (2018) Observed fingerprint of a weakening Atlantic Ocean overturning circulation. Nature, 556(7700):191–196. Publisher: Nature Publishing Group

Cassou C (2008) Intraseasonal interaction between the Madden–Julian oscillation and the North Atlantic Oscillation. Nature, 455(7212):523–527. Number: 7212 Publisher: Nature Publishing Group

Cerato G, Bellomo K, D'Agostino R, von Hardenberg J (2025) Multimodel Evidence of Future Tropical Atlantic Precipitation Change Modulated by AMOC Decline. J Clim 38(13):3093–3107. https://doi.org/10.1175/JCLI-D-24-0333.1

Chemke R, Zanna L, Orbe C, Sentman LT, Polvani LM (2022) The Future Intensification of the North Atlantic winter storm track: the key role of dynamic ocean coupling. *Journal of Climate*, 35(8):2407–2421. Publisher: American Meteorological Society Section: Journal of Climate

Christiansen B (2007) Atmospheric circulation regimes: Can cluster analysis provide the number? J Clim, 20(10):2229–2250. Publisher: American Meteorological Society Section: Journal of Climate

Clark PU, Pisias NG, Stocker TF, Weaver AJ (2002) The role of the thermohaline circulation in abrupt climate change. Nature, 415(6874):863–869. Number: 6874 Publisher: Nature Publishing Group

Corti S, Molteni F, Palmer TN (1999) Signature of recent climate change in frequencies of natural atmospheric circulation regimes. Nature, 398(6730):799–802. Number: 6730 Publisher: Nature Publishing Group

Couldrey MP, Gregory JM, Dong X, Garuba O, Haak H, Hu A, Hurlin WJ, Jin J, Jungclaus J, Köhl A, Liu H, Ojha S, Saenko OA, Savita A, Suzuki T, Yu Z, Zanna L (2023) Greenhouse-gas forced changes in the Atlantic meridional overturning circulation and related worldwide sea-level change. Clim Dyn 60(7):2003–2039

Coumou D, Di Capua G, Vavrus S, Wang L, Wang S (2018) The influence of Arctic amplification on mid-latitude summer circulation. Nat Commun, 9(1):2959. Number: 1 Publisher: Nature Publishing Group

Davini P, D'Andrea F (2020) From CMIP3 to CMIP6: Northern hemisphere atmospheric blocking simulation in present and future climate. J Clim, 33(23):10021–10038. Publisher: American Meteorological Society Section: Journal of Climate

Dawson A (2016) eofs: a library for EOF analysis of meteorological, oceanographic, and climate data. J Open Res Softw, 4(1)

Dawson A, Palmer TN, Corti S (2012) Simulating regime structures in weather and climate prediction models. Geophys Res Lett, 39(21). _eprint: https://onlinelibrary.wiley.com/doi/pdf/10.1029/2012GL053284

Delhaye S, Msadek R, Fichefet T, Massonnet F, Terray L (2023) Consistent but more intense atmospheric circulation response to Arctic sea ice loss in CMIP6 experiments compared to PAMIP experiments. EGUsphere, pages 1–32. Publisher: Copernicus GmbH

Dorrington J, Strommen K, Fabiano F (2022a) Quantifying climate model representation of the wintertime Euro-Atlantic circulation using geopotential-jet regimes. Weather Clim Dyn, 3(2):505–533. Publisher: Copernicus GmbH

Dorrington J, Strommen K, Fabiano F, Molteni F (2022b) CMIP6 models trend toward less persistent European blocking regimes in a warming climate. Geophys Res Lett, 49(24):e2022GL100811. _eprint: https://onlinelibrary.wiley.com/doi/pdf/10.1029/2022GL100811

Drijfhout S, Oldenborgh GJv, Cimatoribus A (2012) Is a Decline of AMOC Causing the Warming Hole above the North Atlantic in Observed and Modeled Warming Patterns? J Clim, 25(24):8373–8379. Publisher: American Meteorological Society Section: Journal of Climate

Döscher R, Acosta M, Alessandri A, Anthoni P, Arsouze T, Bergman T, Bernardello R, Boussetta S, Caron L-P, Carver G, Castrillo M, Catalano F, Cvijanovic I, Davini P, Dekker E, Doblas-Reyes FJ, Docquier D, Echevarria P, Fladrich U, Fuentes-Franco R, Gröger M, v Hardenberg J, Hieronymus J, Karami MP, Keskinen J-P, Koenigk T, Makkonen R, Massonnet F, Ménégoz M, Miller PA, Moreno-Chamarro E, Nieradzik L, van Noije T, Nolan P, O'Donnell D, Ollinaho P, van den Oord G, Ortega P, Prims OT, Ramos A, Reerink T, Rousset C, Ruprich-Robert Y, Le Sager P, Schmith T, Schrödner R, Serva F, Sicardi V, Sloth Madsen M, Smith B, Tian T, Tourigny E, Uotila P, Vancoppenolle M, Wang S, Wårlind D, Willén U, Wyser K, Yang S, Yepes-Arbós X, Zhang Q (2022) The EC-Earth3 Earth system model for the Coupled Model Intercomparison Project 6. *Geoscientific Model Development*, 15(7):2973–3020. Publisher: Copernicus GmbH

Eyring V, Bony S, Meehl GA, Senior CA, Stevens B, Stouffer RJ, Taylor KE (2016) Overview of the Coupled Model Intercomparison Project Phase 6 (CMIP6) experimental design and organization. Geosci Model Dev, 9(5):1937–1958. Publisher: Copernicus GmbH

Fabiano F, Christensen HM, Strommen K, Athanasiadis P, Baker A, Schiemann R, Corti S (2020) Euro-Atlantic weather regimes in the PRIMAVERA coupled climate simulations: impact of resolution and mean state biases on model performance. Clim Dyn 54(11–12):5031–5048

Fabiano F, Meccia VL, Davini P, Ghinassi P, Corti S (2021) A regime view of future atmospheric circulation changes in northern mid-latitudes. Weather Clim Dyn 2(1):163–180

Fox-Kemper B (2021) Ocean, Cryosphere and sea level change. 2021:U13B–09. Conference name: AGU Fall Meeting Abstracts ADS Bibcode: 2021AGUFM.U13B..09F

Frankignoul C, Gastineau G, Kwon Y-O (2013) The influence of the AMOC variability on the atmosphere in CCSM3. J Clim 26(24):9774–9790

Frierson DMW, Hwang Y-T, Fučkar NS, Seager R, Kang SM, Donohoe A, Maroon EA, Liu X, Battisti DS (2013) Contribution of ocean overturning circulation to tropical rainfall peak in the Northern Hemisphere. Nat Geosci, 6(11):940–944. Number: 11 Publisher: Nature Publishing Group

Gastineau G, D'Andrea F, Frankignoul C (2013) Atmospheric response to the North Atlantic Ocean variability on seasonal to decadal time scales. Clim Dyn 40(9):2311–2330

Gervais M, Shaman J, Kushnir Y (2019) Impacts of the North Atlantic Warming hole in future climate projections: mean atmospheric circulation and the North Atlantic Jet. J Clim 32(10):2673–2689

Hall A, Cox P, Huntingford C, Klein S (2019) Progressing emergent constraints on future climate change. *Nature Climate Change*, 9(4):269–278. Publisher: Nature Publishing Group

Hannachi A, Straus DM, Franzke CLE, Corti S, Woollings T (2017) Low-frequency nonlinearity and regime behavior in the

Northern Hemisphere extratropical atmosphere. Rev Geophys, 55(1):199–234. _eprint: https://onlinelibrary.wiley.com/doi/pdf/10.1002/2015RG000509

Harvey BJ, Cook P, Shaffrey LC, Schiemann R (2020) The response of the Northern hemisphere storm tracks and jet streams to climate change in the CMIP3, CMIP5, and CMIP6 Climate Models. J Geophys Res, 125(23):e2020JD032701. _eprint: https://onlinelibrary.wiley.com/doi/pdf/10.1029/2020JD032701

Harvey BJ, Shaffrey LC, Woollings TJ (2014) Equator-to-pole temperature differences and the extra-tropical storm track responses of the CMIP5 climate models. Clim Dyn 43(5):1171–1182

Henry LG, McManus JF, Curry WB, Roberts NL, Piotrowski AM, Keigwin LD (2016) North Atlantic ocean circulation and abrupt climate change during the last glaciation. Science, 353(6298):470–474. Publisher: American Association for the Advancement of Science

...Hersbach H, Bell B, Berrisford P, Hirahara S, Horányi A, Muñoz-Sabater J, Nicolas J, Peubey C, Radu R, Schepers D, Simmons A, Soci C, Abdalla S, Abellan X, Balsamo G, Bechtold P, Biavati G, Bidlot J, Bonavita M, De Chiara G, Dahlgren P, Dee D, Diamantakis M, Dragani R, Flemming J, Forbes R, Fuentes M, Geer A, Haimberger L, Healy S, Hogan RJ, Hólm E, Janisková M, Keeley S, Laloyaux P, Lopez P, Lupu C, Radnoti G, de Rosnay P, Rozum I, Vamborg F, Villaume S, Thépaut J-N (2020) The ERA5 global reanalysis. Q J R Meteorol Soc 146(730):1999–2049

Hochman A, Messori G, Quinting JF, Pinto JG, Grams CM (2021) Do Atlantic-European Weather Regimes physically exist? Geophys Res Lett, 48(20):e2021GL095574. _eprint: https://onlinelibrary.wiley.com/doi/pdf/10.1029/2021GL095574

Horton DE, Johnson NC, Singh D, Swain DL, Rajaratnam B, Diffenbaugh NS (2015) Contribution of changes in atmospheric circulation patterns to extreme temperature trends. *Nature*, 522(7557):465–469. Publisher: Nature Publishing Group

Hoskins B, Woollings T (2015) Persistent extratropical Regimes and climate extremes. Curr Clim Change Rep 1(3):115–124

IPCC (2021). Future Global Climate: Scenario-based Projections and Near-term Information. In Intergovernmental Panel on Climate Change (IPCC), editor, *Climate Change 2021-The Physical Science Basis: Working Group I Contribution to the Sixth Assessment Report of the Intergovernmental Panel on Climate Change*, pages 553–672. Cambridge University Press, Cambridge

Jackson LC, Kahana R, Graham T, Ringer MA, Woollings T, Mecking JV, Wood RA (2015) Global and European climate impacts of a slowdown of the AMOC in a high resolution GCM. Clim Dyn 45(11–12):3299–3316

Keil P, Mauritsen T, Jungclaus J, Hedemann C, Olonscheck D, Ghosh R (2020) Multiple drivers of the North Atlantic warming hole. Nat Clim Change, 10(7):667–671. Publisher: Nature Publishing Group

Lee SH, Tippett MK, Polvani LM (2023) A New Year-Round Weather Regime Classification for North America. J Clim, 36(20):7091–7108. Publisher: American Meteorological Society Section: Journal of Climate

Lee Y-C, Liu W, Fedorov AV, Feldl N, Taylor PC (2024) Impacts of Atlantic meridional overturning circulation weakening on Arctic amplification. Proc Natl Acad Sci, 121(39):e2402322121. Publisher: Proceedings of the National Academy of Sciences

Lin Y-J, Rose BEJ, Hwang Y-T (2023) Mean State AMOC Affects AMOC weakening through subsurface warming in the labrador sea. J Clim, 36(12):3895–3915. Publisher: American Meteorological Society Section: Journal of Climate

Liu W, Fedorov A (2022) Interaction between Arctic sea ice and the Atlantic meridional overturning circulation in a warming climate. Clim Dyn 58(5):1811–1827

Liu W, Fedorov A, Sévellec F (2019) The mechanisms of the Atlantic Meridional overturning circulation slowdown induced by Arctic Sea ice decline. J Clim, 32(4):977–996. Publisher: American Meteorological Society Section: Journal of Climate

Liu W, Fedorov AV, Xie S-P, Hu S (2020) Climate impacts of a weakened Atlantic Meridional Overturning Circulation in a warming climate. Science Advances. American Association for the Advancement of Science, Publisher

Lynch-Stieglitz J (2017) The Atlantic Meridional overturning circulation and Abrupt climate change. *Ann Rev Mar Sci*, 9(Volume 9, 2017):83–104. Publisher: Annual Reviews

Madonna E, Li C, Grams CM, Woollings T (2017) The link between eddy-driven jet variability and weather regimes in the North Atlantic-European sector. Q J R Meteorol Soc 143(708):2960–2972

Meccia VL, Simolo C, Bellomo K, Corti S (2023) Extreme cold events in Europe under a reduced AMOC. *Environmental Research Letters*, 19(1):014054. Publisher: IOP Publishing

Mecking JV, Drijfhout SS (2023) The decrease in ocean heat transport in response to global warming. Nat Clim Change, 13(11):1229–1236. Publisher: Nature Publishing Group

Menary MB, Wood RA (2018) An anatomy of the projected North Atlantic warming hole in CMIP5 models. Clim Dyn 50(7):3063–3080

Michelangeli P-A, Vautard R, Legras B (1995) Weather Regimes: Recurrence and Quasi Stationarity. J Atmosp Sci, 52(8):1237–1256. Publisher: American Meteorological Society Section: Journal of the Atmospheric Sciences

Mimi MS, Liu W (2024) Atlantic Meridional Overturning Circulation slowdown modulates wind-driven circulations in a warmer climate. Commun Earth Environ, 5(1):1–9. Publisher: Nature Publishing Group

Nobre P, Veiga SF, Giarolla E, Marquez AL, da Silva MB, Capistrano VB, Malagutti M, Fernandez JPR, Soares HC, Bottino MJ, Kubota PY, Figueroa SN, Bonatti JP, Sampaio G, Casagrande F, Costa MC, Nobre CA (2023) AMOC decline and recovery in a warmer climate. Sci Rep, 13(1):15928. Publisher: Nature Publishing Group

Oliveira JC, Borchert L, Duchez A, Dobrynin M, Baehr J (2020) AMOC fingerprints influence seasonal SST predictability in the North Atlantic

O'Neill BC, Tebaldi C, van Vuuren DP, Eyring V, Friedlingstein P, Hurtt G, Knutti R, Kriegler E, Lamarque JF, Lowe J, Meehl GA, Moss R, Riahi K, Sanderson BM (2016) The Scenario Model Intercomparison Project (ScenarioMIP) for CMIP6. Geosci Model Dev, 9(9):3461–3482. Publisher: Copernicus GmbH

Oudar T, Cattiaux J, Douville H (2020) Drivers of the Northern Extratropical Eddy-Driven Jet Change in CMIP5 and CMIP6 Models. Geophys Res Lett, 47(8):e2019GL086695. _eprint: https://onlinelibrary.wiley.com/doi/pdf/10.1029/2019GL086695

Palmer TN (1999) A Nonlinear Dynamical Perspective on Climate Prediction. J Clim, 12(2):575–591. Publisher: American Meteorological Society Section: Journal of Climate

Peings Y, Cattiaux J, Vavrus S, Magnusdottir G (2017) Late Twenty-First-Century Changes in the Midlatitude Atmospheric Circulation in the CESM Large Ensemble. J Clim, 30(15):5943–5960. Publisher: American Meteorological Society Section: Journal of Climate

Peings Y, Cattiaux J, Vavrus SJ, Magnusdottir G (2018) Projected squeezing of the wintertime North-Atlantic jet. *Environ Res Lett*, 13(7):074016. Publisher: IOP Publishing

Pfahl S (2014) Characterising the relationship between weather extremes in Europe and synoptic circulation features. Nat Hazards Earth Syst Sci, 14(6):1461–1475. Publisher: Copernicus GmbH

Rahmstorf S (2002) Ocean circulation and climate during the past 120,000 years. Nature, 419(6903):207–214. Number: 6903 Publisher: Nature Publishing Group

Rahmstorf S (2024) Is the atlantic overturning circulation approaching a tipping point? Oceanography 37(3):1

Rivière G (2011) A Dynamical Interpretation of the Poleward Shift of the Jet Streams in Global Warming Scenarios. *J Atmosp Sci*, 68(6):1253–1272. Publisher: American Meteorological Society Section: Journal of the Atmospheric Sciences

Shaw TA, Baldwin M, Barnes EA, Caballero R, Garfinkel CI, Hwang Y-T, Li C, O'Gorman PA, Rivière G, Simpson IR, Voigt A (2016) Storm track processes and the opposing influences of climate change. *Nat Geosci*, 9(9):656–664. Number: 9 Publisher: Nature Publishing Group

Shepherd TG (2014) Atmospheric circulation as a source of uncertainty in climate change projections. *Nat Geosci*, 7(10):703–708. Publisher: Nature Publishing Group

Shepherd TG, Boyd E, Calel RA, Chapman SC, Dessai S, Dima-West IM, Fowler HJ, James R, Maraun D, Martius O, Senior CA, Sobel AH, Stainforth DA, Tett SFB, Trenberth KE, van den Hurk BJJM, Watkins NW, Wilby RL, Zenghelis DA (2018) Storylines: an alternative approach to representing uncertainty in physical aspects of climate change. Clim Change 151(3):555–571

Strommen K, Mavilia I, Corti S, Matsueda M, Davini P, von Hardenberg J, Vidale P-L, Mizuta R (2019) The sensitivity of Euro-Atlantic Regimes to model horizontal resolution. Geophys Res Lett 46(13):7810–7818

Sun L, Deser C, Simpson I, Sigmond M (2022) Uncertainty in the Winter Tropospheric Response to Arctic Sea Ice Loss: The Role of Stratospheric Polar Vortex Internal Variability. J Clim, 35(10):3109–3130. Publisher: American Meteorological Society Section: Journal of Climate

Sévellec F, Fedorov AV, Liu W (2017) Arctic sea-ice decline weakens the Atlantic Meridional Overturning Circulation. Nat Clim Change, 7(8):604–610. Number: 8 Publisher: Nature Publishing Group

Vautard R (1990) Multiple Weather Regimes over the North Atlantic: Analysis of Precursors and Successors. *Mon Weather Rev*, 118(10):2056–2081. Publisher: American Meteorological Society Section: Monthly Weather Review

Weijer W, Cheng W., Garuba OA, Hu A, Nadiga BT (2020) CMIP6 Models Predict Significant 21st Century Decline of the Atlantic Meridional Overturning Circulation. Geophys Res Lett, 47(12):e2019GL086075. _eprint: https://onlinelibrary.wiley.com/doi/pdf/10.1029/2019GL086075

Welch BL (1947) The Generalization of 'Student's' Problem when Several Different Population Variances are Involved. Biometrika, 34(1/2):28–35. Publisher: [Oxford University Press, Biometrika Trust]

Wiel Kvd, Bloomfield HC, Lee RW, Stoop LP, Blackport R, Screen JA, Selten FM (2019) The influence of weather regimes on European renewable energy production and demand. Environ Res Lett, 14(9):094010. Publisher: IOP Publishing

Woollings T (2010) Dynamical influences on European climate: an uncertain future. Philosophical Trans R Soc A 368(1924):3733–3756

Woollings T, Gregory JM, Pinto JG, Reyers M, Brayshaw DJ (2012) Response of the North Atlantic storm track to climate change shaped by ocean-atmosphere coupling. Nat Geosci, 5(5):313–317. Number: 5 Publisher: Nature Publishing Group

Zhang R, Sutton R, Danabasoglu G, Kwon Y-O, Marsh R, Yeager SG, Amrhein D E, Little CM (2019) A Review of the Role of the Atlantic Meridional Overturning Circulation in Atlantic Multidecadal Variability and Associated Climate Impacts. *Reviews of Geophysics*, 57(2):316–375. _eprint: https://onlinelibrary.wiley.com/doi/pdf/10.1029/2019RG000644